*Desalination and Water Treatment*
www.deswater.com
doi: 10.1080/19443994.2015.1044918

57 (2016) 11736–11745
May

Taylor & Francis
Taylor & Francis Group

# Study for adsorption behaviors of emulsion oil on a novel $ZrO_2$/PVDF modified membrane

Xie Xiong[a,b], Bao Jianguo[a,*], Safaa Hassan Omer[a], Guo Hui[a], Zhou Yu[a], Wang Hong[b]

[a]*State Key Laboratory of Biogeology and Environmental Geology, China University of Geosciences, Wuhan 430074, P.R. China, Tel. +18007111908; email: xiexiong77@126.com (X. Xiong), Tel. +0086 27883470; Fax: 0086 27 87436235; email: 18007111908@126.com (B. Jianguo), Tel. +15871404822; email: safaho@yahoo.ca (S. H. Omer), Tel. +18040519731; email: 892450196@qq.com (G. Hui), Tel. +13545039331; email: 474810837@qq.com (Z. Yu)*
[b]*Wuhan Wisco Originwater Environmental Protection Technology Co., Ltd, Wuhan 430074, P.R. China, Tel. +86 13986131701; email: 2825101256@qq.com*

Received 16 October 2014; Accepted 21 April 2015

ABSTRACT

Adsorption is one of the most important reasons for membrane fouling. In this study, adsorption of emulsion oil on a novel $ZrO_2$/PVDF modified membrane and the original PVDF membrane (OM) were compared. The adsorption behaviors between membranes and emulsion oil droplets were investigated by calculating the thermodynamics parameters, fitting adsorption isotherms and kinetic models, in addition to other influencing factors, such as the initial concentration and temperature. The experimental data showed that MM had a better anti-oil-adsorption performance than OM. The results indicated that the Temkin isotherm model was the most suitable to describe emulsion oil adsorption on membranes, which showed that the adsorption tended to be a multilayer adsorption on an inhomogeneous membrane. The thermodynamics parameters showed that physical adsorption was primary, and the adsorption forces between membrane and oil droplets were mainly physical adsorption forces. Moreover, a pseudo-first-order kinetic model produced the highest value of $R^2$, which showed that the emulsion oil adsorption rate on the membrane was directly proportional to the difference in value between the equilibrium concentration and the instantaneous concentration.

*Keywords:* Emulsion oil; Adsorption behavior; Fouling; $ZrO_2$/PVDF membrane

## 1. Introduction

Large volumes of oily wastewater are generated from various industrial processes, such as petrochemical, ferrous metallurgy, pharmacy, food, etc. Because of its ecological hazards, the oily wastewater should be treated before being discharged. Moreover, according to environmental regulations the maximum total oil concentrations for discharge should be below 10–15 mg/L [1]. Industrial oily wastewater can be divided into three main categories: free-floating oil, unstable oil/water emulsions, and stable oil/water emulsions. Free-floating oil and unstable oil emulsions can be easily removed using traditional methods, such as gravity settling, skimming, dissolved air flotation, coalescence, centrifuging, etc. However, for stable emulsions, these methods are ineffective. When the

*Corresponding author.

emulsion oil droplets' size is below 20 μm, it is difficult to separate them from wastewater using conventional techniques [2]. Under such circumstances, membrane technology offers a potential solution to the problem. Ultrafiltration (UF) has been proven to be one of the most efficient ways to separate emulsion oil droplets, but it also has some limitations in practice.

Ceramic membranes play an important role in oil/water separation, but compared with polymer membranes, ceramic membranes are still more expensive and have relatively large pore sizes, which limits their applications. Among all ceramic membranes types, zirconia ceramic membrane is chemically more stable than $TiO_2$ and $Al_2O_3$ membrane [3], and exhibited its superior performance in oily emulsion treatment because of its special surface characteristics, such as high surface density and strong polarity [4]. Nowadays, poly(vinylidene fluoride) (PVDF) has become the most important commercial material for UF membrane because of its comprehensive properties. However, PVDF is more hydrophobic, which may be due to its low surface energy [5]. This hydrophobic nature makes PVDF membrane susceptible to contamination by adsorbed organic pollutants, such as emulsion oil droplets, which may led to severe membrane fouling. In order to improve the anti-fouling property of PVDF membrane, many efforts have been devoted to enhancing the hydrophilicity using different methods, such as surface modification, chemical grafting, physical blending, etc. [6]. Among these methods, the modified polymeric membrane with nanoparticles has become more attractive because of its mild and convenient operation.

Different types of nanoparticles have been used to modify PVDF membrane, such as nanometer titanium dioxide ($TiO_2$) [7], alumina ($Al_2O_3$) [8], silica ($SiO_2$) [9], while so far, zirconia ($ZrO_2$) has been rarely used, and because of the special properties of this material, further potential developments are expected in this field.

The adsorption of pollutant droplets on/in membranes leads to membrane fouling, which may cause serious flux decline. Therefore, many attempts have been made to investigate the adsorption behaviors of membranes with some organic pollutants [10,11]. In our previous study, we used $ZrO_2$ nanoparticles to modify PVDF membrane, and made a novel $ZrO_2$/PVDF modified membrane (MM). To study its application performance in the treatment of low concentration emulsion oily wastewater, it is necessary to investigate its adsorption behaviors with emulsion oil.

The purpose of this paper is to study the static adsorption behaviors of the novel $ZrO_2$/PVDF MM with emulsion oil. In order to illustrate the adsorption effects, the MM was compared with the original PVDF membrane (OM), and the adsorption factors (including initial concentration and temperature), adsorption isotherms, thermodynamic parameters and kinetics behavior were also analyzed systematically.

## 2. Materials and methods

### 2.1. Membranes and characterization

The $ZrO_2$/PVDF MM and the OM used in static adsorption experiments were prepared in our lab with phase inversion method. The properties of the membranes were shown in Table 1.

The crystal structure and the phase composition of $ZrO_2$ nanoparticles, OM and MM were analyzed using X-ray diffraction (XRD) (D/MAX 2550, Japan). A scanning electron microscope (SEM) (FSEM-SU8010, Hitachi, Japan) was used for the investigation of membrane morphology.

### 2.2. Emulsion oily wastewater

The emulsion oily wastewater was prepared as follows: 800 mg engine oil and 100 mg sodium dodecyl sulfate were added to 500 ml deionized water, the solution mixed for 30 min at 3,000 rpm using high speed agitator, and then diluted to 1,000 ml volumetric conical flask. The stable and reproducible emulsion oily wastewater was produced. Fig. 1 showed the emulsion oil droplets' micrograph. Most of the oil droplets were in the range of 0.3–2 μm, the maximum diameter was less than 10 μm, and this simulated wastewater was a typical O/W emulsion wastewater.

### 2.3. Adsorption experiments

Static adsorption experiments were carried out in 500 ml glass conical flasks shaken at constant temperature and 200 rpm in an air bath shaker. A volume of 300 ml emulsion oily wastewater of specific concentration and a piece of membrane with a surface area 50 $cm^2$ were added to the flask, and the adsorption tests were lasted for at least 40 h until the oil concentration in wastewater was stable. In the process, the oil concentration in water was monitored with UV spectrophotometry (Shimadzu, UV2550, Japan) at regular time intervals [12], then the emulsion oil adsorbing amount on membrane should be calculated. By fitting experimental data with adsorption models, the adsorption mechanism could be analyzed, and when compared with original PVDF membrane, the contrastive study of emulsion oil adsorption characteristics on $ZrO_2$/PVDF MM could be conducted.

Table 1
Membrane properties

| Membrane properties | $ZrO_2$/PVDF modified membrane (MM) | Original PVDF membrane (OM) | Determination method |
|---|---|---|---|
| Membrane thickness (μm) | 130–140 | 130–140 | Micrometer |
| Material | PVDF-$ZrO_2$ | PVDF | – |
| Pore diameter (nm) | 50–60 | 50–60 | Guerout–Elford–Ferry equation |
| Contact angle (°) | 69.8 | 76.2 | Water contact angle mesurement |
| Pure water flux ($L/m^2$ h) | 325 | 263 | Filtration experiment (0.1 MPa) |

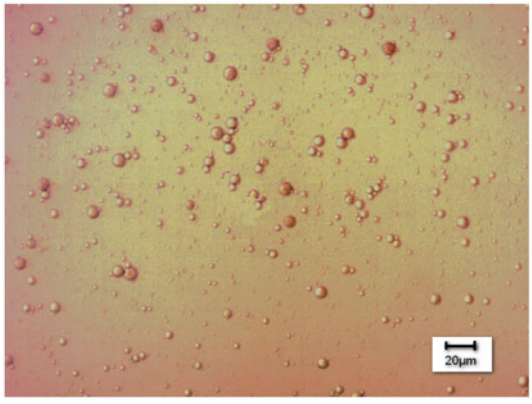


Fig. 1. The micrograph of emulsion oil droplets in wastewater.

### 2.4. Adsorption models

To analyze the experimental data for adsorption behaviors, three classical adsorption isotherm models and four common adsorption kinetics models were used here. The specific equations based on these models can be written as follows:

#### 2.4.1. Adsorption isotherm models

(a) Langmuir model:

$$q = q_{max} \times \frac{K_L.c}{1 + K_L} \quad (1)$$

(b) Freundlich model:

$$q = K_F \times c^n \quad (2)$$

(c) Temkin model:

$$q = a + b \cdot \ln\ c \quad (3)$$

where $q$ is the equilibrium amount of adsorbate adsorbed per unit area of adsorbent; $c$ is the concentration of adsorbate at equilibrium in the solution; $q_{max}$ and $K_L$ are the maximum sorption capacity of the adsorbent in theory and the Langmuir sorption coefficient, respectively. $K_F$ is the Freundlich constant, a measure of sorption capacity of the adsorbent; $n$ is the heterogeneity factor, a constant related to sorption intensity or surface heterogeneity. $a$ and $b$ are two empirical constants in the Temkin model equation.

#### 2.4.2. Adsorption kinetic models

(a) Pseudo-first-order model:

$$Q_t = Q_e(1 - e^{-kt}) \quad (4)$$

(b) Pseudo-second-order model:

$$Q_t = \frac{k \cdot {Q_e}^2 \cdot t}{1 + k \cdot Q_e \cdot t}. \quad (5)$$

(c) Elovich kinetic model:

$$Q_t = A + B \cdot \ln\ t \quad (6)$$

(d) Dual-constant kinetic model:

$$Q_t = e^A \cdot t^B \quad (7)$$

where $Q_t$ is the amount of adsorbate adsorbed at time $t$; $Q_e$ is the saturated adsorption amount; $t$ is the adsorption experimental time; $e$ is Euler's constant; $k$ is the adsorption rate constant, $A$ and $B$ are empirical constants for the associated model equations.

## 3. Results and discussion

### 3.1. XRD analysis and SEM investigation of membranes

The XRD patterns of $ZrO_2$ nanoparticles, OM and MM, are shown in Fig. 2. $ZrO_2$ nanoparticles showed main peaks of $2\theta = 24.5^\circ$, $28.3^\circ$, $31.5^\circ$, and $34.5^\circ$, which agreed with the characteristic peaks of $ZrO_2$ [13]. Fig. 1 also depicts the difference between OM and MM, new peaks (shown with arrows) for $ZrO_2$ could be clearly observed at $2\theta = 24.4^\circ$, $28.2^\circ$, $31.0^\circ$, and $34.2^\circ$ in the XRD pattern of MM. This showed that $ZrO_2$ nanoparticles have been distributed on the PVDF membrane matrix, and the small shift in the peaks' locations illustrated there possibly exist very slight interactions between $ZrO_2$ and PVDF. Similar behaviors have also been seen in the literature for nanoparticles mixed with matrix membranes [14].

Fig. 3 shows the SEM images of the membrane surfaces and cross-sections for OM and MM. It can be seen that OM and MM all exhibited a thin skin layer and large pore structure in the sub-layer, the membrane cross-sections displayed typical asymmetric morphology with finger-like pores linked by sponge walls. Compared with OM, it was easy to find that there were a few $ZrO_2$ nanoparticles dispersed on the surface and cross-section of MM, and the nanoparticles seemed to be relatively well dispersed.

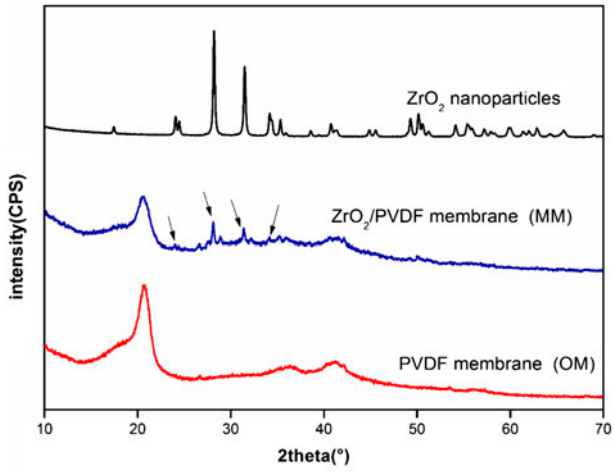


Fig. 2. X-ray patterns of $ZrO_2$ nanoparticles, OM and MM.

### 3.2. Effects of initial concentration and temperature

In Fig. 4, it can be seen that the adsorption tendency of the two membranes (OM and MM) were

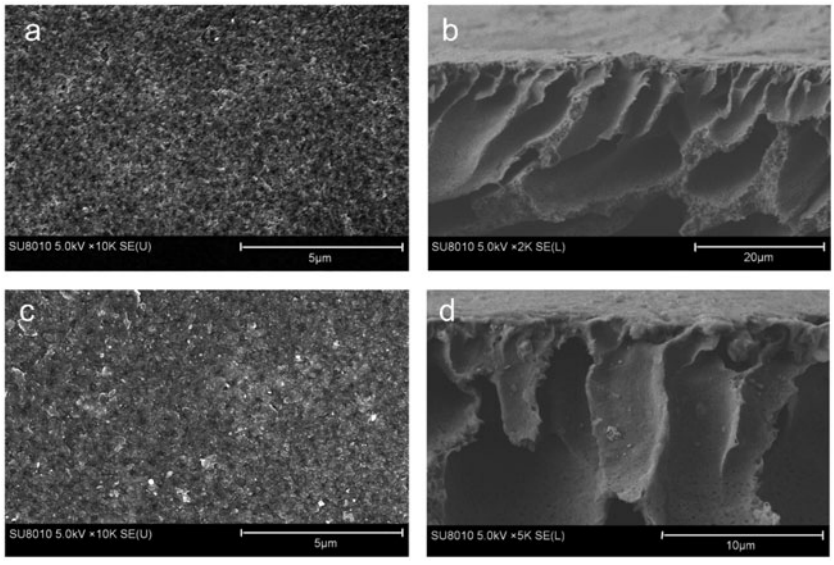


Fig. 3. The SEM images of OM and MM: (a) membrane surface (OM); (b) membrane cross-section (OM); (c) membrane surface (MM); (d) membrane cross-section (MM).

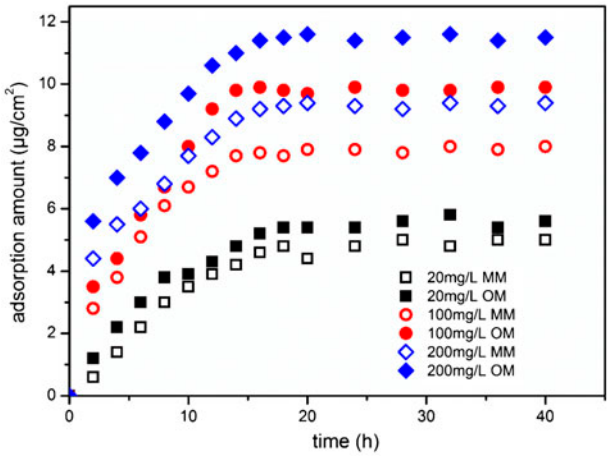


Fig. 4. Effect of oil initial concentration on adsorption amount of OM and MM.

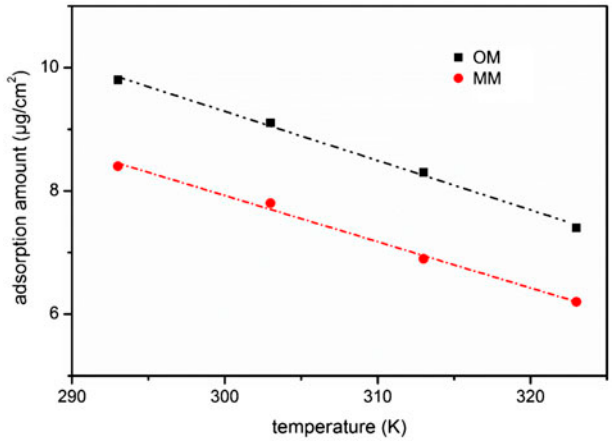


Fig. 5. Effect of temperature on adsorption amount of OM and MM.

nearly identical. For the initial concentrations of emulsion oil of 20, 100, and 200 mg/L, the equilibrium adsorption amounts of OM and MM were 5.6, 9.9, 11.5 and 5, 7.9, 9.4 μg/cm$^2$, respectively. With increased initial concentration, the adsorption amount increased, because of the increase in the mass transfer driving force, but when the adsorption sites were nearly saturated, the adsorption amount did not change greatly. When the initial oil concentration increased from 100 to 200 mg/L, the equilibrium adsorption amount of OM and MM only improved from 9.9 and 7.9 to 11.5 and 9.4 μg/cm$^2$, respectively, and this reflected a net increase in adsorption amount that was far less than the increase of oil concentration in the water, and it showed that a higher oil concentration condition led to a lower adsorption efficiency. This result may be due to the limited adsorption sites of the membrane itself. This phenomenon is similar to the BPA adsorption process on polysulfone membrane under different concentrations, i.e., the higher BPA concentration led to lower adsorption efficiency [11].

In order to investigate the impact of temperature on adsorption performance, a series of experiments was carried out at 293, 303, 313, and 323 K. Fig. 5 shows the oil adsorption amount on the OM and MM at various temperatures. It can be seen that the oil adsorption amount of OM and MM decreased with the increase in temperature. This result showed that the adsorption of oil droplets on the membrane was an exothermic process. The increase in temperature increases the mobility of the emulsion oil droplets, then Brownian motion is accelerated, which led to the result that oil droplets were not easy for the membrane to capture. Therefore, the adsorption amount decreased. This phenomenon showed that increasing the temperature could be beneficial in reducing the oil-adsorption-fouling on membranes in wastewater.

In Figs. 4 and 5, the experimental data shown indicated that the adsorption amount of MM was clearly less than for OM under the same test conditions. These results showed that MM had a better anti-oil-adsorption performance. This indicated that the abundant—OH groups in $ZrO_2$ nanoparticles have significantly improved the hydrophilicity of the membrane surface [3], which weakened the hydrophobic interactions and substantially reduced the deposition of oil droplets.

### 3.3. Fitting adsorption isotherm

Temperature: 303 K; membrane: 50 cm$^2$; contact time: 40 h.

Adsorption isotherms indicate how the adsorbates interact with adsorbents and how adsorption uptake varies with concentration [15]. In Fig. 6, three classical adsorption isotherm models (Langmuir, Freundlich and Temkin equations) were used to fit experimental data by nonlinear regression. It could be seen that the adsorption amounts of emulsion oil on OM and MM increased with increased oil equilibrium concentration, and the increment in oil adsorption amount seemed to be less significant with a further increase of oil equilibrium concentration. The nonlinear fitting parameters for the three adsorption isotherm models are listed in Table 2.

For $q_{max}$ in the Langmuir model, as in Table 2, the obtained values were 11.7672 and 10.1805 μg/cm$^2$ for OM and MM, respectively. In the Freundlich model, the $K_F$ values were 2.8644 and 2.4569, respectively. The data presented by $q_{max}$ and $K_F$ all showed that the

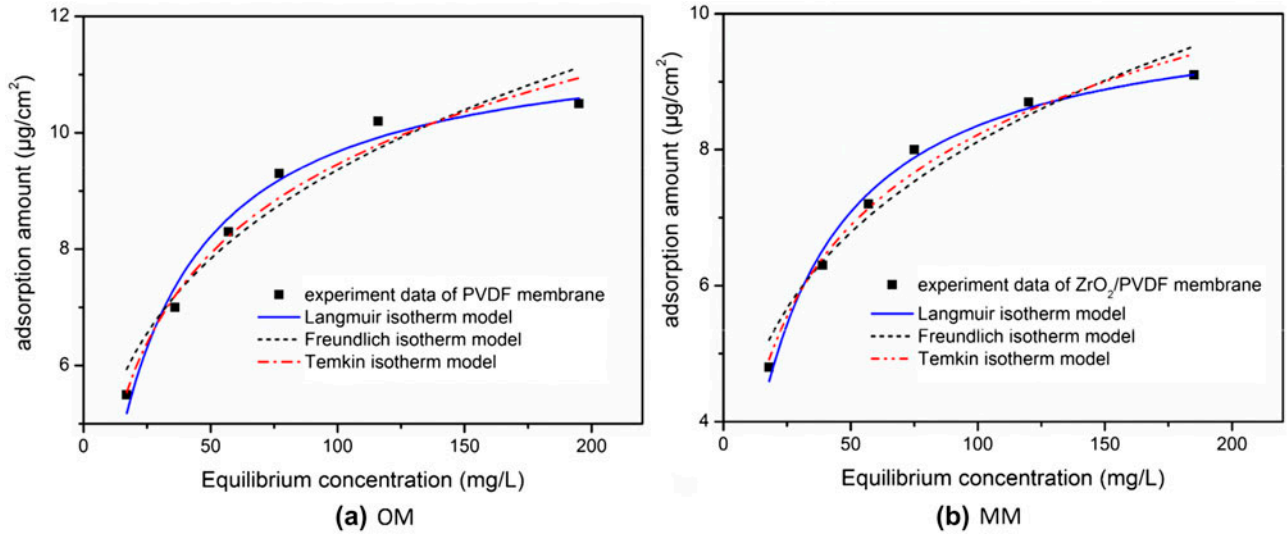


Fig. 6. Emulsion oil adsorption isotherm fitting on OM and MM.

Table 2
Fitting parameters of adsorption isotherm models

| | Langmuir model | | | Freundlich model | | | Temkin model | | |
|---|---|---|---|---|---|---|---|---|---|
| Membrane type | $q_{max}$ | $K_L$ | $R^2$ | $K_F$ | $n$ | $R^2$ | $a$ | $b$ | $R^2$ |
| OM | 11.7672 | 0.0462 | 0.9747 | 2.8643 | 0.2572 | 0.9222 | −0.7338 | 2.1237 | 0.9932 |
| MM | 10.1807 | 0.0457 | 0.9867 | 2.4569 | 0.2595 | 0.9391 | −0.6557 | 1.9274 | 0.9758 |

adsorption amount of oil on MM was less than that on OM under the same conditions. For the Langmuir, Freundlich and Temkin models, the fitting coefficient of determination ($R^2$) had values: 0.9747, 0.9867; 0.9222, 0.9391; and 0.9932, 0.9758 for OM and MM, respectively. The model that had higher values of $R^2$ was considered to be more suitable [16]. Obviously, the results fitted by the Langmuir model and Temkin models were closer to the experimental data than those of the Freundlich model. The Langmuir model is mainly based on monolayer adsorption, but emulsion oil droplets in water are obviously not molecules (as seen in Fig. 1), and oil droplets adsorbed on the membrane surface have an adsorption capacity themselves, they can form multilayer adsorption. By this reasoning, the Temkin model was considered to be more suitable to describe the process than the Langmuir model. However, the $R^2$ values in the Langmuir model were higher than those of the Freundlich model, which showed that the adsorbed oil droplets on the membrane surface tend to spread out to generate an oil film, and this may result in face-to-face membrane fouling. This result agreed with some previous studies [17].

### 3.4. Study thermodynamics parameters

To study the adsorption mechanism further, some related thermodynamic parameters (changes of Gibbs free energy, entropy and enthalpy, as $\Delta_r G_m^\theta, \Delta_r S_m^\theta, \Delta_r H_m^\theta$) were calculated as follows:

Change of Gibbs free energy at any temperature:

$$\Delta_r G_m^\theta = -RT \times \ln K \tag{8}$$

Changes of entropy and enthalpy were calculated by van't Hoff equation:

$$\Delta_r G_m^\theta = -\Delta_r H_m^\theta - T\Delta_r S_m^\theta \tag{9}$$

$$\ln K = \frac{\Delta_r S_m^\theta}{R} - \frac{\Delta_r H_m^\theta}{RT} \tag{10}$$

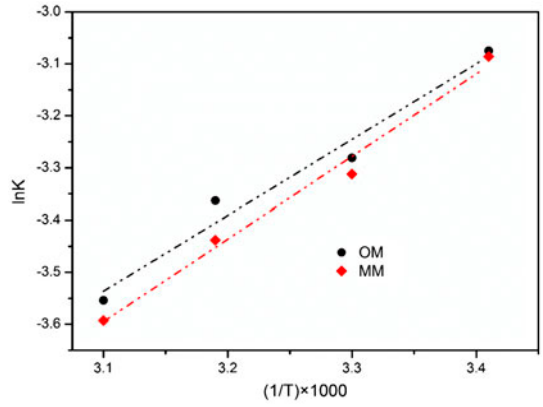


Fig. 7. Van't Hoff equation linear fitting.

where $R$ is the universal gas constant (8.314 J/K·mol) and $T$ is absolute temperature (K). Thus, $\Delta_r S_m^\theta$ and $\Delta_r H_m^\theta$ can be calculated by plotting ln $K$ vs. $1/T$ and fitting a linear equation of the slope and intercept (Fig. 7). The thermodynamic parameters were calculated and are listed in Table 3.

As seen in Table 3, at temperatures of 293, 303, 313 and 323K, $\Delta_r G_m^\theta$ of OM and MM were 7.49, 8.26, 8.75, and 9.54 kJ/mol and 7.52, 8.34, 8.95, and 9.65 kJ/mol, respectively. The obtained results for the two membranes, showed that when the temperature was low, the corresponding $\Delta_r G_m^\theta$ was small, while the absorbability was relatively high, and it showed that the higher temperature did not benefit adsorption. $\Delta_r G_m^\theta$ of OM in comparison with MM at the same temperature was lower than that of MM, which indicated that MM showed relatively poor adsorbability for emulsion oil, therefore, its anti-oil-absorption performance was enhanced.

$\Delta_r H_m^\theta$ and $\Delta_r S_m^\theta$ are independent thermodynamics parameters. The absolute value of $\Delta_r H_m^\theta$ is frequently applied to distinguish physical adsorption and chemical adsorption. Physical adsorption is typically associated with the heats of adsorption in the 5–20 kJ/mol range, while chemical adsorption is typically associated with much larger $\Delta_r H_m^\theta$ values (e.g., 100–400 kJ/mol) [18]. In this study, $\Delta_r H_m^\theta$ values of OM and MM for emulsion oil were −12.09 and −13.17 kJ/mol. $|\Delta_r H_m^\theta|$, which showed that the adsorption of emulsion oil on the two membranes was mainly physical adsorption. It also showed that the adsorption forces between membrane and oil droplets were mainly physical adsorption forces. Furthermore, according to the adsorption heats of different forces (Table 4) determined by Von Oepen et al. [19], the adsorption forces could be attributed to van der Waals force, hydrogen bond and dipole attraction.

### 3.5. Adsorption kinetic analysis

For a clear understanding of the adsorption kinetics process, four common kinetic models (pseudo-first-order, pseudo-second-order, Elovich, and dual-constant models) were adopted to fit the experimental data nonlinearly in Fig. 8, and the fitting parameters are summarized in Table 5.

In Fig. 8, it can be seen at the three different oil concentrations of 20, 100, and 200 mg/L, the oil adsorption amount showed no obvious change after 20 h, which indicates that the adsorption equilibrium time was about 20 h for the membrane-emulsion oil wastewater system. The kinetic curve can be divided into two stages: (1) rapid adsorption stage (0–20 h), in this stage the adsorption amount increased very quickly, it made a major contribution to the equilibrium concentration; (2) a slow adsorption stage (20–40 h), the adsorption amount in this stage increased very slowly, which has a relatively small impact on

Table 3
Adsorption thermodynamics parameters of emulsion oil on OM and MM

| | $\Delta_r G_m^\theta$ (kJ/mol) | | | | | |
|---|---|---|---|---|---|---|
| Membrane type | 293K | 303K | 313K | 323K | $\Delta_r H_m^\theta$ (kJ/mol) | $\Delta_r S_m^\theta$ (J/mol.K) |
| OM | 7.49 | 8.26 | 8.75 | 9.54 | −12.09 | −66.88 |
| MM | 7.52 | 8.34 | 8.95 | 9.65 | −13.17 | −70.72 |

Table 4
The adsorption heat of different force (kJ/mol)

| Van der Waals force | Hydrophobic action | Hydrogen bond | Dentate exchange | Dipole attraction | Chemical bond |
|---|---|---|---|---|---|
| 4–10 | About 3 | 2–40 | About 40 | 2–29 | >60 |

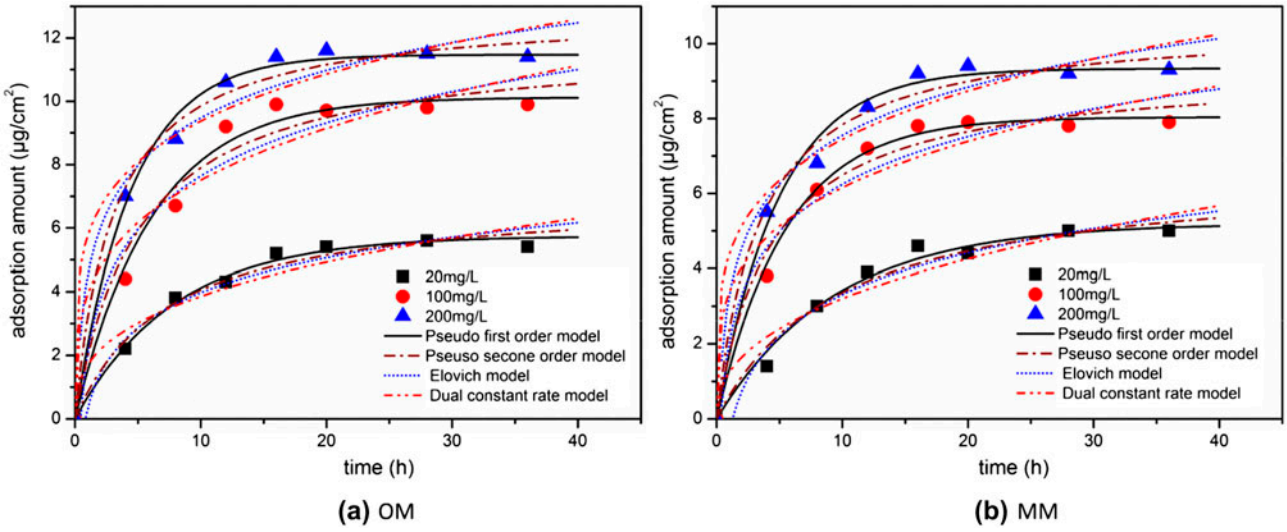


Fig. 8. Adsorption kinetic process fitting on OM and MM at different oil concentrations.

Table 5
Fitting parameters of adsorption kinetic models under different initial concentrations

| Membrane type | Oil concentration (mg/L) | Pseudo first order model | | | Pseudo second order model | | |
|---|---|---|---|---|---|---|---|
| | | $Q_e$ | $k$ | $R^2$ | $Q_e$ | $k$ | $R^2$ |
| OM | 20 | 5.7455 | 0.1261 | 0.9915 | 7.0499 | 0.0192 | 0.9773 |
| | 100 | 10.1258 | 0.1618 | 0.9787 | 11.8932 | 0.0166 | 0.9571 |
| | 200 | 11.4725 | 0.2217 | 0.9735 | 12.8634 | 0.0254 | 0.9806 |
| MM | 20 | 5.1998 | 0.1068 | 0.9790 | 6.6597 | 0.0153 | 0.9596 |
| | 100 | 8.0382 | 0.1801 | 0.9936 | 9.3243 | 0.2453 | 0.9760 |
| | 200 | 9.3369 | 0.2013 | 0.9688 | 10.5626 | 0.0272 | 0.9764 |
| Membrane type | Oil concentration (mg/L) | Elovich model | | | Dual constant rate model | | |
| | | $A$ | $B$ | $R^2$ | $A$ | $B$ | $R^2$ |
| OM | 20 | 0.3082 | 1.5879 | 0.9632 | 0.5315 | 0.3551 | 0.9142 |
| | 100 | 2.0510 | 2.4234 | 0.9268 | 1.3633 | 0.2836 | 0.8876 |
| | 200 | 4.4815 | 2.1682 | 0.9599 | 1.7466 | 0.2131 | 0.9406 |
| MM | 20 | −0.3795 | 1.6010 | 0.9560 | 0.2090 | 0.4139 | 0.8880 |
| | 100 | 2.0177 | 1.8362 | 0.9432 | 1.2117 | 0.2632 | 0.9054 |
| | 200 | 3.2561 | 1.8648 | 0.9598 | 1.4763 | 0.2308 | 0.9404 |

the equilibrium concentration. Then, comparing the fitting parameters of these kinetic models in Table 5, the four models were arranged in order of $R^2$ as below: pseudo-first-order model > pseudo-second-order model > Elovich model > dual-constant model. It is clearly seen that the pseudo-first-order kinetic model had the highest values of $R^2$, showing that the pseudo-first-order model could be more suitable to describe the adsorption kinetic process than other models.

According to the meaning of the pseudo-first-order kinetic model, a preliminary conclusion was drawn that the emulsion oil adsorption rate on the membrane was directly proportional to the difference in value between the equilibrium concentration and instantaneous concentration. Therefore, the adsorption amount

was mainly affected by the diffusion of emulsion oil, which indicates that controlling the diffusion velocity of the emulsion oil could be one of the most effective ways to slow oil adsorption on the membranes.

## 4. Conclusion

Through comparative studies of adsorption for emulsion oil droplets on $ZrO_2$/PVDF MM and the OM, a better understanding of the adsorption behaviors of emulsion oil on the novel $ZrO_2$/PVDF (MM) was obtained. The main conclusions are as follows: (1) For both MM and OM, the adsorption amount increased with increasing initial oil concentration, and decreased when the temperature increased, which was mainly due to the mass transfer driving force and Brownian motion of emulsion oil in water. (2) Among the Langmuir, Freundlich and Temkin isotherm models, the Temkin model was more suitable to fit the experimental data, indicating that the adsorption of emulsion oil on the membrane tended to be multilayer adsorption on an inhomogeneous surface. (3) The results of thermodynamic parameters showed that in the adsorption process, physical adsorption was primary, and the adsorption forces between membrane and oil droplets were mainly physical adsorption forces. (4) Compared with pseudo-second-order, Elovich, and dual-constant kinetic models, the pseudo-first-order model showed the highest values of $R^2$, which showed that the emulsion oil adsorption rate on the membranes was directly proportional to the difference in value between the equilibrium concentration and instantaneous concentration. (5) Moreover, in all experimental data, the equilibrium adsorption amount of oil on MM was less than that on OM, which indicated that MM has a better anti-oil-absorption performance.

## Acknowledgements

This research is supported by the Shenzhen Strategic Emerging Industry Development Special Foundation (grant number JCYJ20130401154122777), JuZheng Environmental Research Fund of China University of Geosciences (Project No. 201203905) and the 2013 key scientific research project of Wisco Engineering and Technology Group Co., Ltd (Project name: The development of oil pollutant resistance membrane).

## References

[1] B. Chakrabarty, A.K. Ghoshal, M.K. Purkait, Ultrafiltration of stable oil-in-water emulsion by polysulfone membrane, J. Membr. Sci. 325 (2008) 427–437.

[2] B. Chakrabarty, A.K. Ghoshal, M.K. Purkait, Cross-flow ultrafiltration of stable oil-in-water emulsion using polysulfone membranes, Chem. Eng. J. 165 (2010) 447–456.

[3] N. Maximous, G. Nakhla, W. Wan, K. Wong, Performance of a novel $ZrO_2$/PES membrane for wastewater filtration, J. Membr. Sci. 352 (2010) 222–230.

[4] J.E. Zhou, Q.B. Chang, Y.Q. Wang, J.M. Wang, G.Y. Meng, Separation of stable oil-water emulsion by the hydrophilic nano-sized $ZrO_2$ modified $Al_2O_3$ microfiltration membrane, Sep. Purif. Technol. 75 (2010) 243–248.

[5] F. Liu, N.A. Hashim, Y.T. Liu, M.R.M. Abed, K. Li, Progress in the production and modification of PVDF membranes, J. Membr. Sci. 375 (2011) 1–27.

[6] L.Y. Ng, A.W. Mohammad, C.P. Leo, N. Hilal, Polymeric membranes incorporated with metal/metal oxide nanoparticles: A comprehensive review, Desalination 308 (2013) 15–33.

[7] F.M. Shi, Y.X. Ma, J. Ma, P.P. Wang, W.X. Sun, Preparation and characterization of PVDF/$TiO_2$ hybrid membranes with different dosage of nano-$TiO_2$, J. Membr. Sci. 389 (2012) 522–531.

[8] X.S. Yi, S.L. Yu, W.X. Shi, S. Wang, L.M. Jin, N. Sun, C. Ma, L.P. Sun, Separation of oil/water emulsion using nano-particle ($TiO_2$/$Al_2O_3$) modified PVDF ultrafiltration membranes and evaluation of fouling mechanism, Water Sci. Technol. 67 (2013) 477–484.

[9] H. Wu, J. Mansouri, V. Chen, Silica nanoparticles as carriers of antifouling ligands for PVDF ultrafiltration membranes, J. Membr. Sci. 433 (2013) 135–151.

[10] H. Song, Y.F. Shi, F. Chao, Oil adsorption measurements during membrane filtration, J. Membr. Sci. 214 (2003) 93–99.

[11] S.H. Wu, B.Z. Dong, Y. Huang, Adsorption of bisphenol A by polysulphone membrane, Desalination 253 (2010) 22–29.

[12] X.S. Yi, W.X. Shi, S.L. Yu, C. Ma, N. Sun, S. Wang, L.M. Jin, L.P. Sun, Optimization of complex conditions by response surface methodology for APAM-oil/water emulsion removal from aqua solutions using nano-sized $TiO_2$/$Al_2O_3$ PVDF ultrafiltration membrane, J. Hazard. Mater. 193 (2011) 37–44.

[13] J.C. Ruiz-Morales, J. Canales-Vázquez, D. Marrero-López, J. Peña-Martínez, A. Tarancón, J.T.S. Irvine, P. Núñez, Is YSZ stable in the presence of Cu? J. Mater. Chem. 18 (2008) 5072–5077.

[14] V. Vatanpour, S.S. Madaeni, A.R. Khataee, E. Salehi, S. Zinadini, H.A. Monfared, $TiO_2$ embedded mixed matrix PES nanocomposite membranes: Influence of different sizes and types of nanoparticles on antifouling and performance, Desalination 292 (2012) 19–29.

[15] M. Min, L. Shen, G. Hong, M. Zhu, Y. Zhang, X. Wang, Y. Chen, B.S. Hsiao, Micro-nano structure poly (ether sulfones)/poly (ethyleneimine) nanofibrous affinity membranes for adsorption of anionic dyes and heavy metal ions in aqueous solution, Chem. Eng. J. 197 (2012) 88–100.

[16] S.M.G. Demneh, B. Nasernejad, H. Modarres, Modeling investigation of membrane biofouling phenomena by considering the adsorption of protein, polysaccharide and humic acid, Colloids Surf., B 88 (2011) 108–114.

[17] A. Hong, A. Fane, R. Burford, Factors affecting membrane coalescence of stable oil-in-water emulsions, J. Membr. Sci. 222 (2003) 19–39.
[18] K. Xu, W.F. Harper, D.Y. Zhao, 17α-Ethinylestradiol sorption to activated sludge biomass: Thermodynamic properties and reaction mechanisms, Water Res. 42 (2008) 3146–3152.
[19] B.V. von Oepen, W. Kördel, W. Klein, Sorption of nonpolar and polar compounds to soils: Processes, measurements and experience with the applicability of the modified OECD-Guideline 106, Chemosphere 22 (1991) 285–304.